This article has been accepted for publication in a future issue of this journal, but has not been fully edited. Content may change prior to final publication. Citation information: DOI 10.1109/JSEN.2020.3040114, IEEE Sensors Journal

Artificial Odour-Vision Synesthesia via Olfactory Sensory Argumentation

Ryan J. Ward, Fred P. M. Jjunju, Elias J. Griffith, Sophie M. Wuerger and Alan Marshall, *Member, IEEE*

***Abstract*— The phenomenology of synaesthesia provides numerous cognitive benefits, which could be used towards augmenting interactive experiences with more refined multisensorial capabilities leading to more engaging and enriched experiences, better designs, and more transparent human-machine interfaces. In this study, we report a novel framework for the transformation of odours into the visual domain by applying the ideology from synaesthesia, to a low cost, portable, augmented reality / virtual reality system. The benefits of generating an artificial form of synesthesia are outlined and implemented using a custom made electronic nose to gather information about odour sources which is then sent to a mobile computing engine for characterisation, classification, and visualisation. The odours are visualised in the form of coloured 2D abstract shapes in real-time. Our results show that our affordable system has the potential to increase human odour discrimination comparable to that of natural synesthesia highlighting the prospects for augmenting human-machine interfaces with an artificial form of this phenomenon.**

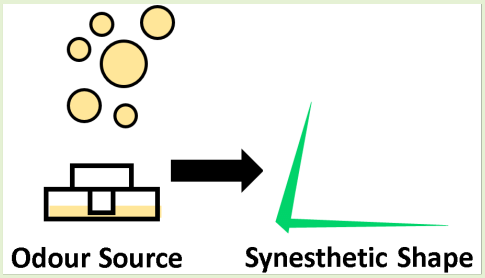

***Index Terms*— Augmented Reality, E-nose, Electronic Nose, Olfaction, Synesthesia, Artificial Synesthesia, Human-machine interface**

I. Introduction

AROMAS are embedded into our everyday life; from the rich smell of freshly ground coffee to the fresh aroma after a summers rain. Despite the ubiquity of olfactory stimuli, the human perception of the olfactory stimulus is still not fully understood [1]. Olfactory perception varies significantly and is influenced by cultural factors, social factors, sex, age, memory, past experiences, and emotions [2]. The olfactory stimulus has the most variability among humans compared to any other sense and can act as a powerful memory stimulant [3]. Human classification of odours can be a complicated task, contemplating the fact there are more than 1000 types of olfactory receptors and humans can discriminate, at most, one trillion different odours [1], making discrimination easy, but identification difficult. The detection and classification of aromas can be a difficult task for humans, albeit elementary for an electronic nose (e-nose). E-noses can discriminate complex odours but are customarily fine-tuned to solve specific problems, such as wine classification [4], lung cancer screening [5], and diabetes diagnosis [6]. Like the human olfactory stimulus, e-noses are based on an array of gas sensors, where each gas sensor has a limited capability of detection and its specificity comes from the quantity of sensors. E-noses often rely on pattern recognition systems for the characterisation and classification of odour sources, rather than the output from a specific sensor [7] and does not rely on the chemical composition of an aroma. As such, projecting information from the olfactory stimulus to another more readily understood in real time would prove to be beneficial for human in the loop odour localisation, feature identification, information recall, and human cognition. This study focuses on the latter.

The coupling of different senses naturally occurs in the neurological condition known as synesthesia, which affects approximately 1 in 2000 people [8]. This phenomenon, broadly speaking, occurs when stimulation in one sensory modality causes unusual, albeit unexpected output in another modality [9]. Synesthetes sometimes possess superior cognitive benefits relating to their form of synaesthesia [10]–[12]. Synesthetes with odour to vision synesthesia have been shown to have a consistent and increased sensitivity for odour and colour discrimination, as well as the correct identification of odours [12]. A small body of research [13]–[15] has shown that it is possible to replicate the phenomenology of synesthesia in non-synesthetes. Although it is still not fully understood if the cognitive benefits of synestheisia can be artificially replicated and to what extent.

Some forms of artificial synesthesia have been investigated; Plouznikoff *et al.* [14] created a head-mounted display that replicates grapheme-colour synesthesia, their results suggest that short term memory recall (digit matrices) and visual information search times can be improved. Konishi *et al.* [16] created a suit capable of augmenting the traditional

This work was supported in full by EPSRC under Grant EP/P004040/1.

R. J. Ward, F. P. M. Jjunju, E. J. Griffith and A. Marshall is with the Department of Electrical and Electronic Engineering, University of Liverpool, Liverpool, 9 Brownlow Hill, L69 7ZX, UK (e-mail: ryan.ward, fjjunju, ejg and alanm@liverpool.ac.uk).

S. M. Wuerger is with the Department of Psychology, University of Liverpool, Liverpool, Eleanor Rathbone Building, L69 7ZA, UK (e-mail: sophiew@liverpool.ac.uk)

This work is licensed under a Creative Commons Attribution 4.0 License. For more information, see https://creativecommons.org/licenses/by/4.0/

This article has been accepted for publication in a future issue of this journal, but has not been fully edited. Content may change prior to final publication. Citation information: DOI 10.1109/JSEN.2020.3040114, IEEE Sensors Journal

visual audio paradigm with haptics, this suit has 26 vibrating actuators that are triggered by soundwaves. Foner [17] created a system that converts light into sound, this allows for the sonification of both perceivable and unperceivable sources of light, allowing for the detection of camouflage in a forest environment. Most of the work in this area focuses on augmenting human-computer interfaces with information outside of the range of human perception, which is comparable with sensory argumentation devices. Meijer created "the vOICe" [18] that converts multiple visual properties (luminance, vertical and horizontal position) to the auditory properties (pitch, frequency, and amplitude), which is consequently presented to a human user. Prolonged usage of this device has invoked synesthetic like experiences [19], [20] in some individuals. Kerdegari *et al.* [21] created a tactile helmet for firefighters that presents navigation commands via tactile feedback. This uses an ultrasound sensor to provide depth information sequentially relaying information to the actuators situated inside the helmet of the firefighter. The sensory experience perceived by humans is rather limited in the sense that we only perceive a small portion of it, these devices open up opportunities to expand upon and build new "senses" for humans. The concept of "artificial synesthesia" will allow for the subtle presentation of information between the real and virtual worlds, while minimising functional and sensory overload providing an overt, low attention human-machine interface using real-world information [22].

In this paper, we report an affordable system for the synesthetic visualisation of odour sources in real-time using a low cost, custom made and portable electronic nose and a mobile computing engine. We then explore to see if our artificial odour-vision synaesthesia provides the same benefit as natural odour-vision synesthesia by testing if odour discrimination is improved when an abstract and complementary visual representation is provided. The experimental system consists of an odour detector (e-nose), a pattern recognition system for the creation of distinct colour profiles, and a visualiser element. Sixteen aromatic oil samples were atomised in the open air using a piezoelectric transducer based olfactory display. First, a benchtop commercial mass spectrometer coupled using an ambient ionisation source (DAPCI) was used to detect and profile the different odours of the atomised aromatic samples with high sensitivity and specificity in an open environment [23], [24], and secondly using a custom-built e-nose with a lesser sensitivity and specificity but with the advantage of being low-cost and portable. A random forest classifier was used to generate distinct colour profiles and a data visualisation algorithm was created to turn the odours transduced by the e-nose into a coloured 2D abstract shape that represents the current odour source. An offline version of the system was then implemented to determine if the system could increase human odour discrimination that is comparable to that of natural odour-vision synesthesia.

II. Materials & Methods

A. Chemicals and Reagents

Sixteen Mystic Moments^{TM} aromatic oils were used in the confines of these experiments; banana, black pepper, cedarwood, caramel, coffee, euculyptus, fudge, lemon, lime, orange, patchouli, tea tree, vanilla and ylang ylang. These were chosen as they were deemed to have a 'perceptual overlap' in some cases to the authors of this paper and were readily available. The samples used in the experiments consist of 4.5 mL of deionized water combined with 0.5 mL of the respective oils with a ratio of 9:1 (v/v).

B. Participants

Twelve individuals (4 female and 8 males with a mean age of 36) took part in the experiment. No participants declared any olfactory impairments (issues that affect the sense of smell, such as, a cold or flu). The experiment took approximately 20 minutes with a 10 minute break half way though to prevent olfactory fatigue. Ethical approval was obtained from the University of Liverpool and conducted in accordance with the standards set in the Declaration of Helsinki for Medical Research Involving Human Subjects. Participants gave written consent before taking part in the experiment.

C. Instrumentation

The system consists of three elements (as shown in Fig. 1): (A) an active odour source (olfactory display), (B) an odour detector (chemical sensor(s)), (C) A mobile computing engine with a pattern recognition system and a visualiser. The odour detection subcomponent (Fig. 1 (B)) transduces the detected odour and sends packets to a router, which then forwards the packets to the mobile computing engine, which sequentially applies a calibration frame to the raw sensor data. This is then passed to the pattern recognition system (Fig. 1 (C)) followed by the synesthetic shape generator, for the colouring and vertex generation respectively.

D. Aroma Generation

A piezoelectric transducer was used for the generation of different aromas (Fig. 1 (A)), this was attached to a small circular container (6.5cm x 3cm) that contains the aromatic solution. The transducer consists of a piezoelectric plate (Seeed Studio) that heats the aromatic solution using ultrasound and has a frequency of 105 ± 5 kHz. This creates a vertical bottom-up diffusion to produce a fine mist. As one aroma was released at any given time, a single piezoelectric transducer was used, but to avoid contamination, the transducer was cleaned with cotton wool and new container was used for each aromatic solution. The aromatic solution placed within the container, consists of half the created solution (2.5 mL) and was refilled to the same volume for each recording. The solution was left sitting in the container for at least 10 minutes to allow the cotton sliver to absorb the solution. A mount was created to house the piezoelectric transducer and the cotton sliver, shown in Fig. S1. To minimise odour plume turbulent, the aromas were released in a controlled environment with restricted external airflow. This room was also flushed with clean air for a minimum of twenty minutes between samples to reduce contamination. Odours were not pretreated (i.e., temperature and humidity control) as we wanted to present them to the e-nose the same manner as how a human would perceive them to create a "perceptual overlap".

This work is licensed under a Creative Commons Attribution 4.0 License. For more information, see https://creativecommons.org/licenses/by/4.0/

This article has been accepted for publication in a future issue of this journal, but has not been fully edited. Content may change prior to final publication. Citation information: DOI 10.1109/JSEN.2020.3040114, IEEE Sensors Journal

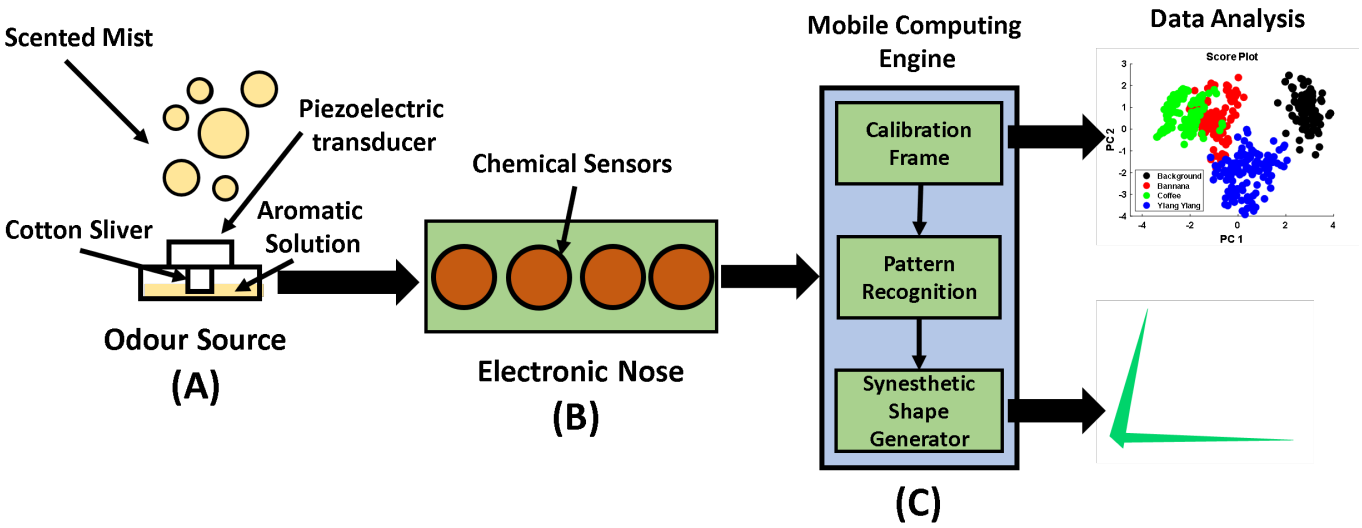

Fig. 1. Schematic representation of the complete system for our olfactory sensory argumentation system.

E. Mass Spectrometry

All mass spectrometry experiments were performed using desorption atmospheric pressure chemical ionisation mass spectrometry (DAPCI MS) on a Xevo triple quadrupole mass spectrometer (TQ MS) (Waters Corporation, Manchester, UK) operated in positive ion mode using previously optimised parameters for the molecular ion of interest. Full mass spectrometry scan mode was used with a mass acceptance window of 50 to 400 Dalton (Da). The source temperature was maintained at 100°C. The cone voltage was set to 50 V, optimised to attain good transmission of ions in the range of interest (50 – 400 amu). The DAPCI ion source was place approx. 3 mm away from the inlet of the mass spectrometer while the aroma generator was placed in close proximity with the DAPCI ion source $\approx$ 4 cm.

F. Electronic Nose

The electronic nose (Fig. 1 (B)) was built at the Immersive Reality Laboratory (University of Liverpool). The sensor array contains five commercially available gas sensors; MP503, BME680, MQ3, MQ5 and WSP2110 (Seeed Studio) designed to detect a wide range of odours (Table 1) and not just those in the confines of these experiments. The sensor array was connected to an Arduino MKR1000 microcontroller (mouser.co.uk) and controlled using custom software. The sensor array was mounted into a chamber, aromas were guided though this chamber and the average output resistance of each sensor was taken as a response. This is then sent to the mobile computing engine (Fig. 1 (C)) using user datagram protocol (UDP) $\approx$ every 125 ms. The schematic for the e-nose is shown in Fig. S2. The calibration frame in the mobile computing engine (Fig. 1 (C)) consists of taking the absolute difference between the averaged background sensor response over 30 seconds (background subtraction [25]) and sequentially taking the median value for each sensor response after applying a moving average over a 1 second interval. The e-nose was flushed with ambient air for a minimum of twenty minutes between uses.

Gas Sensor Name	Detection Range (ppm)	Most Sensitive Gases	Sensor Output Name
MP503	10 - 1,000	Alcohol & Smoke	Air Quality & Temperature
BME680	0 - 500	IAQ	Humidity, Pressure & Gas
MQ3	0.05 - 10	Alcohol & Benzine	MQ3
MQ5	200 - 10,000	LPG, Natural Gas Town Gas, Alcohol & Smoke	MQ5
WSP2110	1 - 50	Toluene, Methanol, Benzene, Alcohol & Acetone	HCHO

TABLE I
GAS SENSORS WITH THEIR RANGE AND DETECTABLE GASES. THE INFORMATION IN THIS TABLE WAS OBTAINED FROM THE CORRESPONDING SENSORS' DATASHEET.

G. Data Analysis

The data analysis was conducted using MATLAB^{TM} R2018b. The recordings obtained for the data analysis and the pattern recognition system consist of 8 columns, one for each sensor response from the electronic nose, each recording is a minute in length. Measurements were repeated 5 times for each odour, with a total of 70 prepared for the experiments. The e-nose was situated 20 cm away from the odour source, this distance was chosen as it gave a good response for our model odour (banana) which allowed for controlled characterisation of each odour. The e-nose was placed (10 cm, 20 cm, 30 cm and 40 cm) away from the aroma generator; an optimal signal was achieved at 20 cm away from the e-nose and this distance was then used in all experiments. To simulate a rising intensity the outtake of the e-nose was switched off during the odour recordings and was only turned on to clean the sensor chamber. Random forest, k-nearest neighbour and a support

This work is licensed under a Creative Commons Attribution 4.0 License. For more information, see https://creativecommons.org/licenses/by/4.0/

This article has been accepted for publication in a future issue of this journal, but has not been fully edited. Content may change prior to final publication. Citation information: DOI 10.1109/JSEN.2020.3040114, IEEE Sensors Journal

vector machine, were trained and tested after applying the calibration frame to the raw sensor data. Random forest was consequently chosen as it had the best performance; the trained model was then used to generate the colour for the synesthetic shape generator. These algorithms were chosen as they are commonly used to classify data from e-noses [25]–[28] and are sufficiently lightweight to be efficiently implemented on a device with limited processing power.

H. Olfactory Visualisation

A custom augmented reality system was created for this experiment and consists of an inexpensive head mounted display (Noon VR™, [29]) chosen for its ability to mount a mobile phone without obstructing the view of the camera. A (Sony™ Xperia Z1, [30]) was used for the mobile computing engine (Fig. 1 (C)). This algorithm was developed to partially exploit heterogeneous response underlying an e-nose signal and from each given sensor to create a 2D abstract shape that represents the current odour source. Typically real-time e-nose responses are visualised as a radar graph also referred to as a polar plot or a bar chart [25], we believed that this representation of the underlying data was not unique enough for the task at hand. The mobile computing engine was programmed in C# using Unity 2018.3.0f and uses the following algorithm to generate the vertices coordinates.

$$x_i = \frac{1}{1 + \sigma_i \sin(\frac{2\pi i}{\frac{m_1 m_2}{9} + \frac{\sigma_i}{2}})}, \text{ for i = 1, 2, 3,... n} \quad (1)$$

$$y_i = \frac{1}{1 + \sigma_i \tanh(\frac{2\pi i}{\frac{m_1 m_2}{9} + \frac{\sigma_i}{2}})}, \text{ for i = 1, 2, 3,... n} \quad (2)$$

Where n is the number of sensor responses from the electronic nose, σ_i is the current value from sensor(i), m_1 and m_2 is the index location for the first and second largest values in the vector respectively. x_i and y_i correspond to the vertex coordinates centred around the origin on a Cartesian plane.

III. Results & Discussion

A. Odour Detection

First, odours were recorded in the open environment using tandem mass spectrometry (MS/MS) in positive ion mode with DAPCI coupled to a commercial mass spectrometer. These experiments were performed to determine the optimum odour detection method. To confirm the identity and the active chemical compounds of each aromatic oil tandem mass spectrometry (MS/MS) was used. The active compound(s) of interest were detected and isolated using collision induced tandem mass spectrometry (MS/MS) [31]. Three model compounds were chosen, due to their presence in a wide variety of aromas these are; phenyl alcohol, methyl butyrate and allyl hexanoate. Intense protonated ions [M+H] for each sample were obtained, as shown in Fig. 2, these CID fragment peaks for the standard model compounds confirm structure of the model compounds.

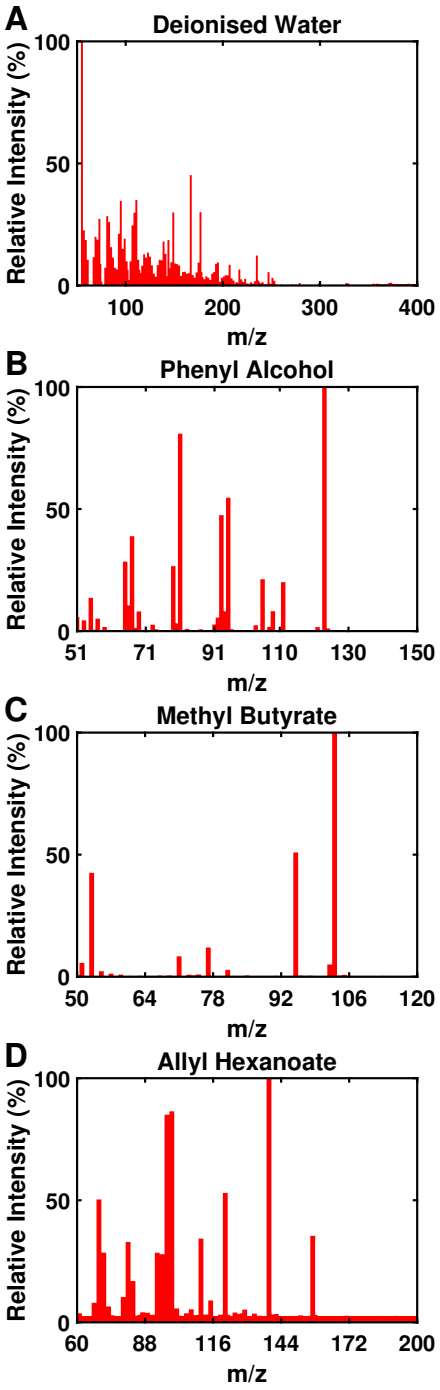

Fig. 2. Positive ion mod DAPCI-MS collision induced (CID MS/MS) mass spectras; phenyl alcohol (**B**) (Mw 122), methyl butyrate (**C**) (Mw 102) and ally hexanoate (**D**) (Mw 156), protonated ion molecules [M+H]+ at m/z 157, 117, 152 and 103.

Representative mass spectrum's of the aromatic oil samples was recorded using DAPCI-MS $\approx$ 10 μL of each sample was spotted on the piezoelectric transducer and analysed using a commercial mass spectrometer. The mass spectra recorded for the aromatic oil samples (banana, coffee and ylang ylang) and a mass spectrum for deionised water is shown in Fig. S3. Sample responses for the e-nose using the aromatic oil samples is shown in Fig. S4. The solutions for the range of detection using the e-nose consist of 500 ppm of the respective

This work is licensed under a Creative Commons Attribution 4.0 License. For more information, see https://creativecommons.org/licenses/by/4.0/

This article has been accepted for publication in a future issue of this journal, but has not been fully edited. Content may change prior to final publication. Citation information: DOI 10.1109/JSEN.2020.3040114, IEEE Sensors Journal

model compound in deionised water, is shown in Fig. 3. This revealed that the e-nose can detect and therefore characterise a wide variety of aromas and not just the ones chosen in the confines of this experiment, however, with less sensitivity and specificity compared to DAPCI-MS. Although DAPCI-MS provides higher sensitivity and specificity there are certain trade-offs that make this solution of odour detection unfeasible. First and foremost, lack of access to the data in real-time and the cost of the solution, consequently, going against the goal of making olfaction more accessible to humans in real-time. In contrast the e-nose offers a cheap lightweight solution for the real-time detection of odour sources, there is a unique response pattern for each detectable aroma, allowing for the discrimination between odour sources. It is important to note that the pretreatment of chemicals is not essential for e-nose systems as it relies on the response patterns rather than the direct output of the sensors', although in some cases the chemicals would need to be pretreated dependant of the task of the e-nose.

B. Principal Component Analysis

Factor analysis using Principal Component Analysis (PCA) was conducted on the sample aromatic oils (banana, coffee and ylang ylang). First a dataset was constructed using the median sensor response after applying a moving average over 1 second intervals. This was done for all five recordings for background, banana, coffee and ylang ylang, using the last twenty five seconds of each recording. The dataset was then logged and underwent z-score normalisation using the population standard deviation and standardised against independent features (gas sensor responses). We decided to use the last twenty five seconds because the first twenty seconds of each recording was ambient air (no odour), additionally we allowed an extra fifteen seconds for the odour to diffuse into the environment and be presnted to the e-nose. The first three principal components explain 80.21% of the total variance, 43.24%, 22.08% and 14.87% respectively. The first two components are shown in the score plot Fig. 4A, we can see that there is overlap between the different odours, but each odour has its own unique range which provides a 'fingerprint' for the identification of odours. This overlap between the odours allow for the generation of consistent and distinct colour profiles for each odour. The inclusion of the third principal component did not visually improve separation.

From the loadings plot Fig. 4B we can see intensity plays an important part in the separation of the odours shown in Fig. 4A, that is the loadings plot suggests that the intensity component is the most contributory factor for explaining the variation in the x axis. It is therefore likely that the intensity of an odour plays the most contributory role in the colour and shape variation of the system. It also shows that the air quality sensor (BME 680) is the most responsive sensor in our array towards the detection of our fragrant oils. The intensity variable corresponds to the time in which each odour has been spent being transduced by our olfactory display and was included to visualise the role it plays in the synesthetic shape generator subcomponent.

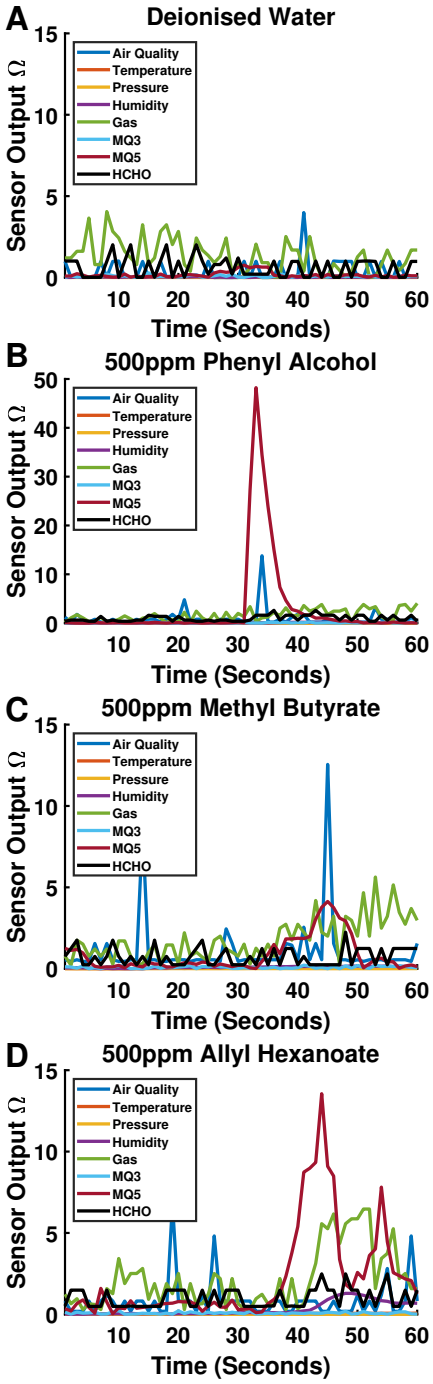

Fig. 3. Sample e-nose responses for the standard model compounds and deionised water, samples were spotted on the piezoelectric transducer for the limit of detection.

C. Pattern Recognition

Out of the 15 aromatic oils, 10 were used to train the pattern recognition system (banana, caramel coffee, eucalyptus, lemon, orange, patchouli, tea tree, vanilla and ylang ylang) with the addition of the background samples, for a total of 11 classes. The last 30 seconds of each recording were used to construct a dataset, and consists of only the pre-processed sensor responses. This dataset was then programmatically split into two for training and testing a variety of machine learning

This work is licensed under a Creative Commons Attribution 4.0 License. For more information, see https://creativecommons.org/licenses/by/4.0/

This article has been accepted for publication in a future issue of this journal, but has not been fully edited. Content may change prior to final publication. Citation information: DOI 10.1109/JSEN.2020.3040114, IEEE Sensors Journal

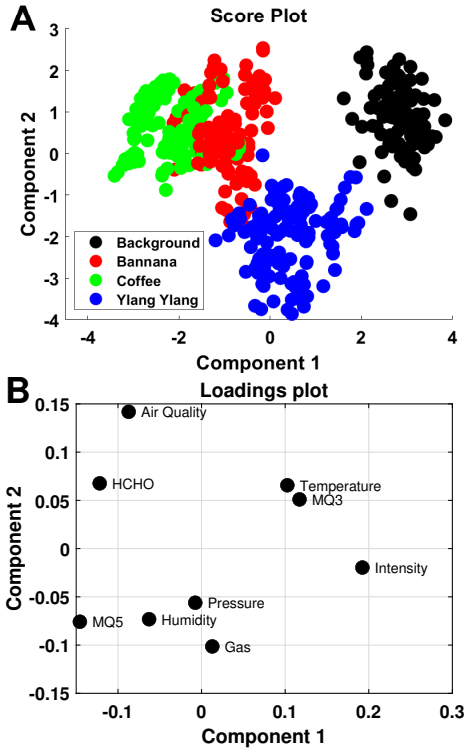

Fig. 4. Score plot (A) of 3 different odours and the background response from the e-nose after pre-processing and the loadings plot. Loadings (PCA coefficients) plot (B) shows the correlation coefficients. Both the score plot (A) and loadings plot (B) are based on the PCA correlation matrix.

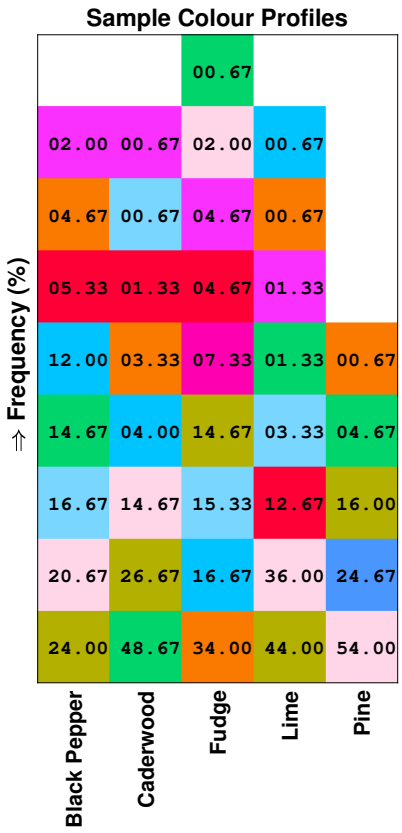

Fig. 5. Sample colour profiles for unknown aromatic oils. Frequency of each colour is the number of of many times the colour occurred in 150 seconds of recordings for each odour indicated as a percentage.

methods, random forest, support vector machine and k-nearest neighbour. All algorithms were trained and tested using 50-fold cross validation, the dataset was randomly split in 50 groups, 49 groups were used for training and 1 group for testing, this process was repeated 50 times until all groups had been tested. The accuracy ratings are: 95.57%, 95.0% and 88.6% for random forest, SVM and kNN respectively. The discrimination ability of the pattern recognition system may be improved by including a more diverse range and/or calibrating the sensor array for specific gases. Sample colour profiles for aromatic oils not used in the training stage (black pepper, cederwood, fudge, lime and pine) are shown in, Fig 5. A one-one mapping between the class output and colour was implemented to assign a colour to the shape. Ten interpolated points were taken from the outside of a cylindrical representation of the L*a*b* colour space at (L* = 70). The L*a*b* colour space [32] was used because of its perceptual uniformity, this allowed the selection for colours deemed to be equally spaced apart perceptually. We assigned the colour black to be the colour of the background (no odour) class.

D. Olfactory Visualisation

The mobile computing engine programmatically assigns a visual representation of the current odour source and super-imposes it onto a live feed of the subjects' camera, as shown in Fig. 6A. The augmented reality aspect is combined with a stereoscopic view of the real-world scene (AR/VR), to allow the user to move around the environment unhindered. The visualiser fuses the data from the e-nose and the pattern recognition system to create a 2D abstract shape the represents the current odour source Fig. 6B-D. This uses the sensor responses from the e-nose after applying the calibration frame. The abstract shape was designed for the ambient abstract visualisation of odour sources to loosely resemble real odour-vision syneasthesia, to show the potential of augmenting an artificial form of syneathesia in human-machine interfaces. The visual representation of the odour source consists using sensor data from the e-nose after applying the calibration frame and undergoing the algorithm shown in Eq. (1) and (2). This then transforms the one dimensional vector into a two dimensional shape, the same 1 dimensional vector is provided as input into the pattern recognition system which determines the colour of the shape.

Fig. 7. shows five different shapes generated from the same recording (cederwood) with a rising intensity, from this we can see as the odours' intensity increases the more consistent the colour and the shape generated by the system gets. This compliments the findings from the PCA loadings plot Fig. 4B, that suggests the intensity is the most influential factor, considered together this indicates a strong relationship between the intensity of odour and the generated shape.

E. Odour Discrimination Experiment

In this experiment, an offline version of the system was developed to avoid environmental contamination. The samples

This work is licensed under a Creative Commons Attribution 4.0 License. For more information, see https://creativecommons.org/licenses/by/4.0/

This article has been accepted for publication in a future issue of this journal, but has not been fully edited. Content may change prior to final publication. Citation information: DOI 10.1109/JSEN.2020.3040114, IEEE Sensors Journal

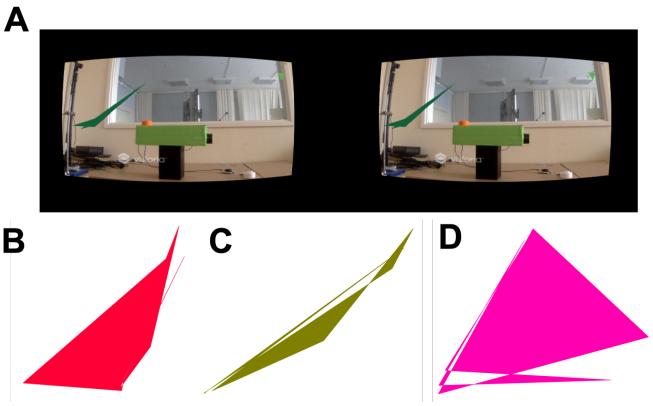

Fig. 6. (A) Sample output of the system while recording the aroma cederwood. (B, C, D) Sample shape generated by the system for banana, coffee and ylang ylang respectively.

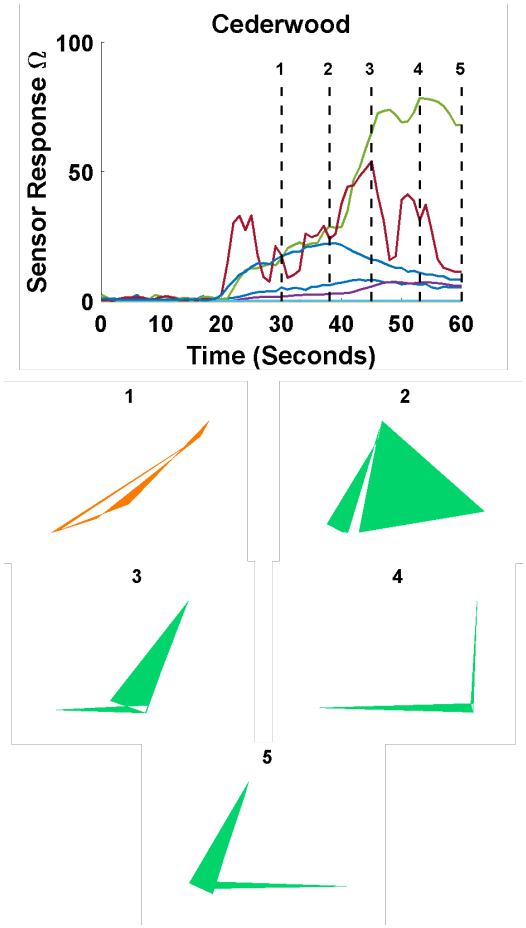

Fig. 7. Sample shapes and colours generated over time with a rising intensity for the cederwood aroma. 1 - 5 shows the coloured shape generated at 30, 37, 45, 52 and 60 seconds respectively.

consisted of 200 μL of the respective aromatic oil (16 in total) placed on a 3cm x 1cm cotton sliver. This was then sealed in a polypropylene test tube. The samples were then covered in white tape and numbered, a total of 27 (9 triplet groupings) were prepared for this experiment. Participants (N = 12) performed an odour discrimination task, they were presented triplets of odours in a random permutation, and modelled after "Sniffin Sticks" [33]. Participants were untrained with use of the system and were simply asked to discriminate between the triplets of odours using their sense of smell and their sense of smell with the abstract shape. Participants were restricted to a maximum of 5 seconds when smelling each odour and was done twice, first with no visual aid and second with the coloured shape pre-generated by the system. Fig. 8 shows that artificial emulation of odour-vision synaesthesia increases odour discrimination, a one-tailed paired t-test with a Bonferroni correct alpha of α = 0.0042 = (0.05 / 12) was conducted to see if the performance increase was statistically significant. This revealed that use of the system increased odour discrimination than without $t(11)$ = -5.84, $p < 0.001$ and has a mean increase of 32.40%. This task had a chance performance of 3.7% to get 100% correct, although the participants were instructed to use their sense of smell along with the visual aid we can not be sure if they solely used one sense as opposed to both.

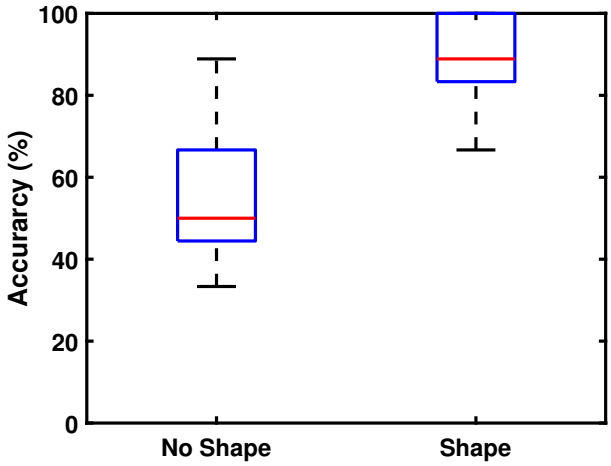

Fig. 8. Boxplot showing the median (red line), the minimum and maximum values (black horizontal lines) and 25th and 75th percentiles indicated by the bottom and top edges (blue box) respectively.

These results show that our system could enhance human odour discrimination in a simple task, which is comparable to that of natural synesthesia [12]. Although more prolonged usage of the system will need to be conducted to determine if the artificial emulation of odour-vision synesthesia can facilitate colour discrimination, odour identification and the extent of odour discrimination. Although designed to be complementary, operation without using the human olfactory stimulus can also be accomplished and might enhance information recall when coupled with olfaction enhanced tasks [34], [35]. The system also emulates some of the characteristics of real syneasthesia in the sense that it is passive, real-time, and perceived to be argumentation on the users' visual field.

IV. Conclusion

We developed an olfactory sensory argumentation device based upon an affordable electronic nose and a smartphone for visualisation. The results revealed that using data fusion we gain the possibility to represent complex odours in the visual

This work is licensed under a Creative Commons Attribution 4.0 License. For more information, see https://creativecommons.org/licenses/by/4.0/

This article has been accepted for publication in a future issue of this journal, but has not been fully edited. Content may change prior to final publication. Citation information: DOI 10.1109/JSEN.2020.3040114, IEEE Sensors Journal

domain in real-time in the form of a 2D abstract shape and that applying the ideology of synesthesia to human-machine interfaces can provide overt, low attention and transparent interfaces with the benefits closely resembling the advantages of its natural counterpart. A sensory test revealed that use of our system can significantly enhance human odour discrimination in a simple task. Thus the proposed solution can help augment interactive experiences with more refined multisensorial capabilities leading to more engaging and enriched experiences, better designs, and more transparent human-machine interfaces. As well as, providing a framework for human in the loop odour localisation, real-time feature identification (e.g., [36], [37]), enhanced information recall, and improved human cognition (e.g., [38]). We hypothesise that these shape and colour mappings could be learnt over time with usage of the system (increasing both olfactory identification and colour discrimination, see [12]), similar to sensory substitution systems (i.e., [39]) where participants learnt to associate sound patterns to images from the real world.

REFERENCES

[1] R. C. Gerkin and J. B. Castro, "The number of olfactory stimuli that humans can discriminate is still unknown," *eLife*, vol. 4, no. JULY 2015, pp. 1–15, 2015.

[2] G. Ghinea and O. A. Ademoye, "Olfaction-enhanced multimedia: perspectives and challenges," *Multimedia Tools and Applications*, vol. 55, no. 3, pp. 601–626, 2011.

[3] S. Chu, "Odour-evoked Autobiographical Memories: Psychological Investigations of Proustian Phenomena," *Chemical Senses*, vol. 25, no. 1, pp. 111–116, 2000.

[4] M. Aleixandre, J. Lozano, J. Gutiérrez, I. Sayago, M. Fernández, and M. Horrillo, "Portable e-nose to classify different kinds of wine," *Sensors and Actuators B: chemical*, vol. 131, no. 1, pp. 71–76, 2008.

[5] W. Li, H. Liu, D. Xie, Z. He, and X. Pi, "Lung Cancer Screening Based on Type-different Sensor Arrays," *Scientific Reports*, vol. 7, no. 1, 2017. [Online]. Available: www.nature.com/scientificreports/

[6] W. Ping, T. Yi, X. Haibao, and S. Farong, "A novel method for diabetes diagnosis based on electronic nose," *Biosensors and Bioelectronics*, vol. 12, no. 9-10, pp. 1031–1036, 1997.

[7] J. W. Gardner and P. N. Bartlett, "A brief history of electronic noses," *Sensors and Actuators: B. Chemical*, vol. 18, no. 1-3, pp. 210–211, 1994.

[8] S. Baron-Cohen, L. Burt, F. Smith-Laittan, J. Harrison, and P. Bolton, "Synaesthesia: Prevalence and familiality," *Perception*, vol. 25, no. 9, pp. 1073–1079, 1996.

[9] E. M. Hubbard and V. S. Ramachandran, "Neurocognitive mechanisms of synesthesia," *Neuron*, vol. 48, no. 3, pp. 509–520, 2005.

[10] D. Brang, L. E. Miller, M. McQuire, V. S. Ramachandran, and S. Coulson, "Enhanced mental rotation ability in time-space synesthesia," *Cognitive Processing*, vol. 14, no. 4, pp. 429–434, 2013.

[11] V. C. Gross, S. Neargarder, C. L. Caldwell-Harris, and A. Cronin-Golomb, "Superior encoding enhances recall in color-graphemic synesthesia," *Perception*, vol. 40, no. 2, pp. 196–208, 2011.

[12] L. J. Speed and A. Majid, "Superior olfactory language and cognition in odor-color synaesthesia," *Journal of Experimental Psychology: Human Perception and Performance*, vol. 44, no. 3, pp. 468–481, 2018.

[13] D. Bor, N. Rothen, D. J. Schwartzman, S. Clayton, and A. K. Seth, "Adults can be trained to acquire synesthetic experiences," *Scientific Reports*, vol. 4, 2014. [Online]. Available: http://audacity.sourceforge.net

[14] N. Plouznikoff, A. Plouznikoff, and J. M. Robert, "Artificial grapheme-color synesthesia for wearable task support," in *Proceedings - International Symposium on Wearable Computers, ISWC*, vol. 2005. IEEE, 2005, pp. 108–111.

[15] J. Ward and P. Meijer, "Visual experiences in the blind induced by an auditory sensory substitution device," *Consciousness and Cognition*, vol. 19, no. 1, pp. 492–500, mar 2010. [Online]. Available: http://dx.doi.org/10.1016/j.concog.2009.10.006

[16] Y. Konishi, N. Hanamitsu, B. Outram, K. Minamizawa, T. Mizuguchi, and A. Sato, "Synesthesia suit: the full body immersive experience," in *ACM SIGGRAPH 2016 VR Village*, 2016, pp. 1–1.

[17] L. N. Foner, "Artificial synesthesia via sonification: A wearable augmented sensory system," *Mobile Networks and Applications*, vol. 4, no. 1, pp. 75–81, 1999.

[18] P. B. Meijer, "An Experimental System for Auditory Image Representations," *IEEE Transactions on Biomedical Engineering*, vol. 39, no. 2, pp. 112–121, 1992.

[19] J. Ward and P. Meijer, "Visual experiences in the blind induced by an auditory sensory substitution device," *Consciousness and cognition*, vol. 19, no. 1, pp. 492–500, 2010.

[20] P. Fletcher, "Seeing with sound: A journey into sight," *Retrieved September*, vol. 21, p. 2015, 2002.

[21] H. Kerdegari, Y. Kim, and T. J. Prescott, "Head-mounted sensory augmentation device: Designing a tactile language," *IEEE transactions on haptics*, vol. 9, no. 3, pp. 376–386, 2016.

[22] A. Plouznikoff, N. Plouznikoff, J.-M. Robert, and M. Desmarais, "Enhancing human-machine interactions: Virtual interface alteration through wearable computers," in *Proceedings of the SIGCHI Conference on Human Factors in Computing Systems*, 2006, pp. 373–376.

[23] R. G. Cooks, Z. Ouyang, Z. Takats, and J. M. Wiseman, "Ambient mass spectrometry," *Science*, vol. 311, no. 5767, pp. 1566–1570, 2006.

[24] F. P. Jjunju, S. Maher, A. Li, A. K. Badu-Tawiah, S. Taylor, and R. Graham Cooks, "Analysis of polycyclic aromatic hydrocarbons using desorption atmospheric pressure chemical ionization coupled to a portable mass spectrometer," *Journal of the American Society for Mass Spectrometry*, vol. 26, no. 2, pp. 271–280, 2015.

[25] S. M. Scott, D. James, and Z. Ali, "Data analysis for electronic nose systems," *Microchimica Acta*, vol. 156, no. 3-4, pp. 183–207, 2006.

[26] H. Liu, Q. Li, B. Yan, L. Zhang, and Y. Gu, "Bionic electronic nose based on mos sensors array and machine learning algorithms used for wine properties detection," *Sensors*, vol. 19, no. 1, p. 45, 2019.

[27] Y. Luo, W. Ye, X. Zhao, X. Pan, and Y. Cao, "Classification of data from electronic nose using gradient tree boosting algorithm," *Sensors (Switzerland)*, vol. 17, no. 10, p. 2376, 2017.

[28] F. J. Acevedo, S. Maldonado, E. Domínguez, A. Narváez, and F. López, "Probabilistic support vector machines for multi-class alcohol identification," *Sensors and Actuators, B: Chemical*, vol. 122, no. 1, pp. 227–235, 2007.

[29] "Noon VR." [Online]. Available: http://www.noonvr.eu/

[30] "Sony Xperia Z1 - Full phone specifications." [Online]. Available: https://www.gsmarena.com/sony_xperia_z1-5596.php

[31] F. W. Mclafferty, "Tandem Mass Spectrometry (MS/MS): A Promising New Analytical Technique for Specific Component Determination in Complex Mixtures," *Accounts of Chemical Research*, vol. 13, no. 2, pp. 33–39, 1980.

[32] M. R. Luo, *"Encyclopedia of Color Science and Technology"*. New York, NY: Springer New York, 2016, pp. 207–212.

[33] G. Kobal, T. Hummel, B. Sekinger, S. Barz, S. Roscher, and S. Wolf, "" sniffin'sticks": screening of olfactory performance." *Rhinology*, vol. 34, no. 4, p. 222, 1996.

[34] G. Ghinea and O. A. Ademoye, "Olfaction-enhanced multimedia: Bad for information recall?" in *2009 IEEE International Conference on Multimedia and Expo*. IEEE, 2009, pp. 970–973.

[35] O. A. Ademoye and G. Ghinea, "Information recall task impact in olfaction-enhanced multimedia," *ACM Transactions on Multimedia Computing, Communications, and Applications (TOMM)*, vol. 9, no. 3, pp. 1–16, 2013.

[36] Z. Ouyang and R. G. Cooks, "Miniature mass spectrometers," *Annual Review of Analytical Chemistry*, vol. 2, pp. 187–214, 2009.

[37] D. T. Snyder, C. J. Pulliam, Z. Ouyang, and R. G. Cooks, "Miniature and fieldable mass spectrometers: recent advances," *Analytical chemistry*, vol. 88, no. 1, pp. 2–29, 2016.

[38] R. J. Ward, S. Wuerger, and A. Marshall, "Smelling sensations: olfactory crossmodal correspondences," *bioRxiv*, 2020.

[39] M. Auvray, S. Hanneton, and J. K. O'Regan, "Learning to perceive with a visuo-auditory substitution system: Localisation and object recognition with 'The vOICe'," *Perception*, vol. 36, no. 3, pp. 416–430, 2007.

This work is licensed under a Creative Commons Attribution 4.0 License. For more information, see https://creativecommons.org/licenses/by/4.0/